



Physikalisch-Technische Bundesanstalt
Braunschweig und Berlin

The following article is hosted by PTB;
DOI: 10.7795/810.20240206 It is provided for personal use only.

On-site Measurement and Comparison of Passive Intermodulation generated from different RF absorbers

A. Sayegh, K.Kuhlmann, F. Gellersen, and T. Kleine-Ostmann

Acknowledgement: The authors thank the Federal Ministry for Digital and Transport, Germany (BMDV) for funding this project titled “5GReallabor in der Mobilitätsregion Braunschweig-Wolfsburg”. We also acknowledge Mr. Ohms from deutsche Telekom for borrowing us the radiating antenna.

Available at:

<https://doi.org/10.7795/810.20240206>

On-site Measurement and Comparison of Passive Intermodulation generated from different RF absorbers

Ahmed Sayegh, Karsten Kuhlmann, Frauke Gellersen, Thomas Kleine-Ostmann

Physikalisch-Technische Bundesanstalt (PTB)
Braunschweig, Germany, 38116
Ahmed.Sayegh@PTB.de

ABSTRACT

The accurate measurement of Passive intermodulation (PIM) generated from RF radiating components requires an interference-free environment. The anechoic chamber environment is a suitable option to avoid any external interference that may disturb the PIM measurement. However, RF absorbers in anechoic chambers can be a potential source of PIM and thus affect the measurement accuracy. This paper presents a detailed evaluation of PIM performance for five kinds of absorbers from different manufacturers. It is confirmed that some RF absorbers can be a potential source of PIM. The obtained results show that the conductive carbon material used in fabricating the WAVASORB® VHP-8 absorber, EHP-5PCL absorber and MWA-LFA produces low level of PIM. The nano-metal films incorporated inside Frankonia absorber produces lower PIM compared to carbon-made absorbers. Lastly, the absorber made from EVU material (dry mix of cellulose materials, carbon fibers and other components) produces a higher PIM level.

INTRODUCTION

The rapid increase of high-speed devices has resulted in huge demand for high capacity, low latency, large bandwidth and reliable communication systems [1, 2]. For that purpose, the RF receivers of base stations must be able to detect the weak RF data signals of the mobile high-speed devices. Unfortunately, passive intermodulation (PIM) signals can compromise the receiver sensitivity and thus degrade the performance of the communication systems [3, 4]. So, it is essential to test PIM of the passive RF components in accordance with the IEC62037-1 standard [5] before using them in the communication system.

Basically, PIM is created by mixing two or more RF signals. When these signals pass through a nonlinear component such as a nonlinear contact [6] or nonlinear materials [7]. The non-radiative PIM testing of RF passive devices such as RF connectors and filters is less prone to the external interference signals in the environment. Unfortunately, the PIM test of radiating RF devices such as antennas is strongly affected by external disturbances existing in the test environment [8]. Therefore, radiative PIM tests should be performed in interference-free environments, such as anechoic chambers.

Although PIM testing in an anechoic chamber can greatly improve the accuracy of the measurement result, RF absorbers are one of the most important components that can contribute to the result [9]. This can be attributed to the material type used to fabricate the absorber. In [10], an evaluation and comparison of PIM produced from two different types of absorbers is presented. This paper follows a similar approach, investigating absorbers from five different manufacturers in terms of PIM performance as well as including power sweeps.

The measurement setup, measurement procedure and measurement results are presented in the next sections.

DESCRIPTION OF THE MEASUREMENT SETUP

In this work, the reflected PIM measurement method is adopted for measuring the radiated PIM generated by RF absorbers under test (AUT). As shown in Fig. 1, the measurement setup consists of scalar PIM site analyzer (PIA) from Rosenberger, a dual-band sector antenna placed on a wooden support, a wooden structure for holding the AUT and an aluminum sheet as a reflective surface behind the AUT. Five different types of absorbers are tested, and their specifications are described in Table 1. A sample of WAVASORB® VHP-8 absorber is provided by E&C Anechoic Chambers. It is made from a conductive carbon material and the typical power reflectivity at 2.1 GHz is around -35 dB. The absorber sample footprint is 610 mm x 610 mm, and the total height is 203 mm. The number of pyramids is 81. Fig. 2 (a). shows a sample of WAVASORB® VHP-8 absorber while it is attached to the holding structure during the measurement.

Table 1. Specification of the AUT

Absorber manufacturer	Absorber Model	Absorber shape	Absorber sample dimensions	Given letter	Number of Pyramids	Additional Info
E&C Anechoic Chambers	WAVASORB® VHP-8	Pyramidal	610 mm x 610 mm x 203 mm	A	81	Carbon loaded urethane foam absorber
X	XYZ	Pyramidal	600 mm x 600 mm x 320 mm	B	36	EVU (dry mix of cellulose materials, carbon fibers and other components)
ETS-Lindgren	EHP-5PCL	Pyramidal	600 mm x 600 mm x 127 mm	C	144	urethane foam impregnated with a conductive carbon
Frankonia	HPP 60	Pyramidal	610 mm x 610 mm x 660 mm	D	9	Carbon-free, nano-metal films incorporated inside the absorber
MTC Micro Tech Components	MWA-LFA-610x610x12,7-N	Flat sheet	610 mm x 610 mm x 12.7 mm	E	-	carbon loaded lossy Foam Absorbers

The second AUT is made from EVU material. EVU material is formed by dry mixing of stable components with cellulose materials and carbon fibers. The power reflectivity of this AUT is -40 dB at 2.1 GHz. The AUT footprint is 600 mm x 600 mm while the total height is 320 mm. A photo of this absorber sample, while it is attached to the wooden structure, is given in Fig. 2 (b).

The absorber sample from ETS-Lindgren is fabricated of urethane foam impregnated with conductive carbon. The absorber footprint is 610 mm x 610 mm, and the base height is 25 mm while the overall height is 127 mm. The power reflectivity of this AUT is around -30 dB.

The absorber sample from Frankonia is made using Frankosorb technology where the nano metal film is deposited on non-combustible dielectric sheets [11]. The total overall height of the sample is 660 mm, while the AUT footprint is 610 mm x 610 mm. The power reflectivity is less than -40 dB. Fig. 2 (c) shows a sample of this tested absorber while it is in the measurement setup. The power reflectivity of this AUT is -40 dB at 2.1 GHz.

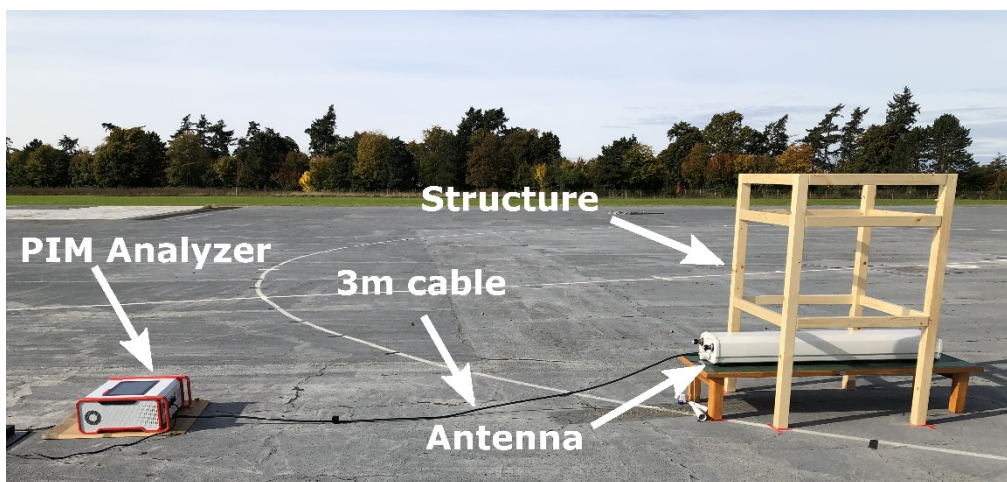


Fig. 1. Photo of the measurement setup in the field.

A flat absorber sample is provided by MTC Micro Tech Components. It is made from polyether foam with a conductive carbon material. The footprint of this AUT is 610 mm x 610 mm while the height is 12.7 mm. A sample of this absorber during the measurement is shown in Fig. 2 (d). The power reflectivity of this AUT is -28 dB at 2.1 GHz.

A support structure of 720 mm width, 720 mm length and 1335 mm height has been built entirely from wood to minimize creation of PIM from the test setup itself. As depicted in Fig. 2 (a), an aluminum sheet is centered on top of the structure

behind the absorber, to create a reflective surface. The distance between the antenna and the AUT is varied by using three testing positions. The distance between the antenna radiating surface and the base of the AUT is 850 mm, 750 mm and 650 mm in Positions #1, #2 and #3, respectively.

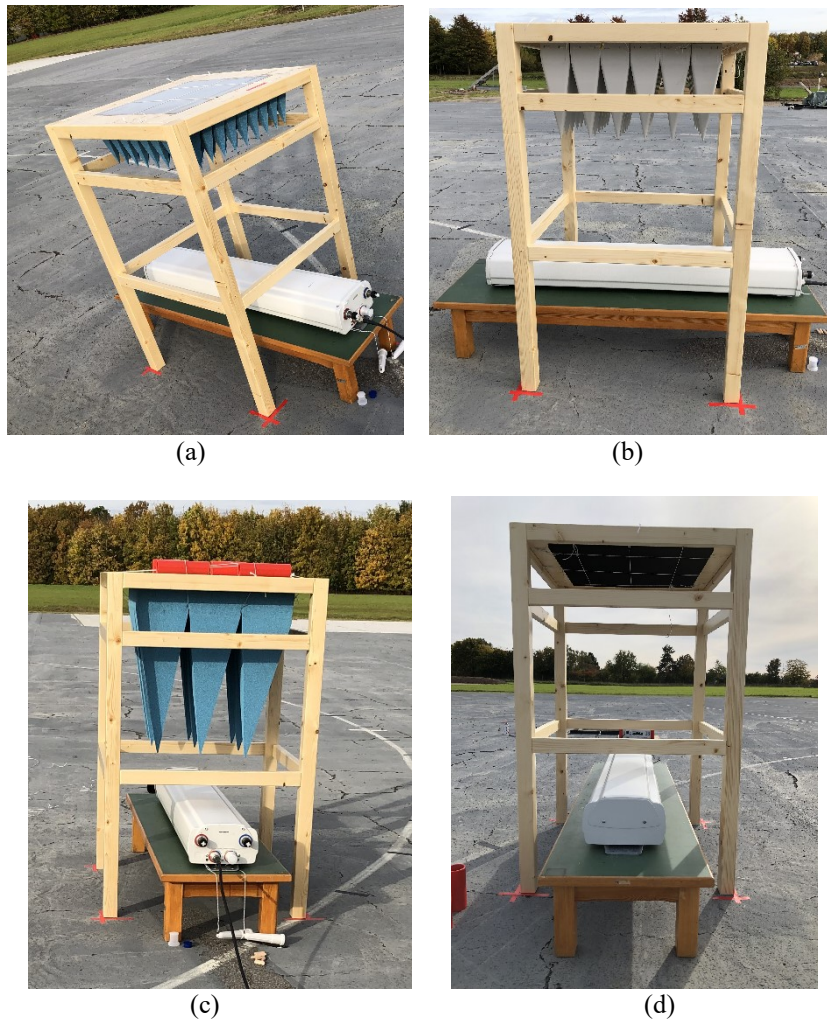


Fig. 2. Samples of the tested absorbers (a) WAVASORB VHP-8 (b) EVU material-made absorber (c) HPP 60 absorbers (d) MTC-MWA-LFA- 610 mm x 610 mm x 12.7 mm.

DESCRIPTION OF THE MEASUREMENT PROCEDURE

The measurements are performed in an open area test site located at Physikalisch-Technische Bundesanstalt (PTB), Germany. This test site is Europe's largest open area test site with dimensions of 50 m x 60 m. It is built in a remote area where there are no buildings in the vicinity to minimize the impact of the external interference on the measurement. At this location, external RF sources which might interfere with the measurements are found to be low. For PIM testing, the PIM analyzer is set to generate a two-tone test signal at frequency $f_1 = 2110$ MHz and frequency $f_2 = 2170$ MHz with 43 dBm carrier power each. The duration time of the PIM measurement is set to 30 seconds. Only the 3rd PIM product ($2f_1 - f_2 = 2050$ MHz) was measured, since it is the strongest one. The RF receiver is set to average mode and the measured parameters are PIM vs. time and PIM vs. two-tone power.

Before the actual measurement, the PIM analyzer is connected to a low-PIM load using a test cable, to verify that the return loss and the residual PIM of the measurement system are within acceptable limits. Next, the far-end of the testing cable is disconnected from the low-PIM load and connected to the testing antenna. The return loss and the generated PIM are then measured. After that, the PIM analyzer is operated in the receiving mode to check for interference signals within the measurement frequency range.

The antenna is positioned to radiate towards the sky and the wooden structure is placed centrally above the antenna. The return loss and the generated self-intermodulation are measured. For the actual measurement, the AUT is placed at Position#1 and the return loss and generated PIM are measured. The same procedure has been repeated for all samples and the generated PIM in all positions is measured. The results are analyzed and a comparison of PIM performance of all the absorbers is evaluated as shown in the next section.

RESULTS AND DISCUSSION

Results of PIM versus Time at Position#1

In this measurement, the two-tone power is set to 43 dBm each. The tone#1 frequency is 2110 MHz while tone#2 frequency is set to 2170 MHz and only the 3rd PIM product is measured. At first, the residual PIM of the measuring system (analyzer, cable, low PIM load) is measured, and it is around -135.7 dBm. After that, the residual PIM versus time for the whole set-up (PIM analyzer, cable, antenna, structure, reflective surface) is measured and the result is shown in Fig. 3 with letter 'F'.

Next, the AUTs are attached to the structure ceiling at Position#1 and the PIM versus time for all the samples is measured and results are shown in Fig. 3. It is found that the HPP60 absorber from Frankonia (Absorber D) which is fabricated using Frankosorb technology produces low PIM values between -135 dBm and -140 dBm compared to the other tested absorbers. The conductive carbon material which is used in manufacturing WAVASORB® VHP-8 absorber (Absorber A) produces low PIM slightly more than the PIM produced from Frankosorb technology absorbers. The conductive carbon material in EHP-5PCL absorber (Absorber C) produces low PIM as well around -130 dBm. In addition to that, the conductive carbon material used in fabricating the MWA-LFA absorber from MTC Micro Tech Components (Absorber E) generates slightly Low PIM around -122 dBm which is the highest PIM among the caron-made AUT. The last type of the tested absorber is built from EVU material which produces high level of PIM (around -62 dBm), as illustrated in Fig. 3 (Absorber B) below. It is important to mention that Absorber 'B' is tested with its metallic holder. However, it still produces high PIM even without that metallic holder.

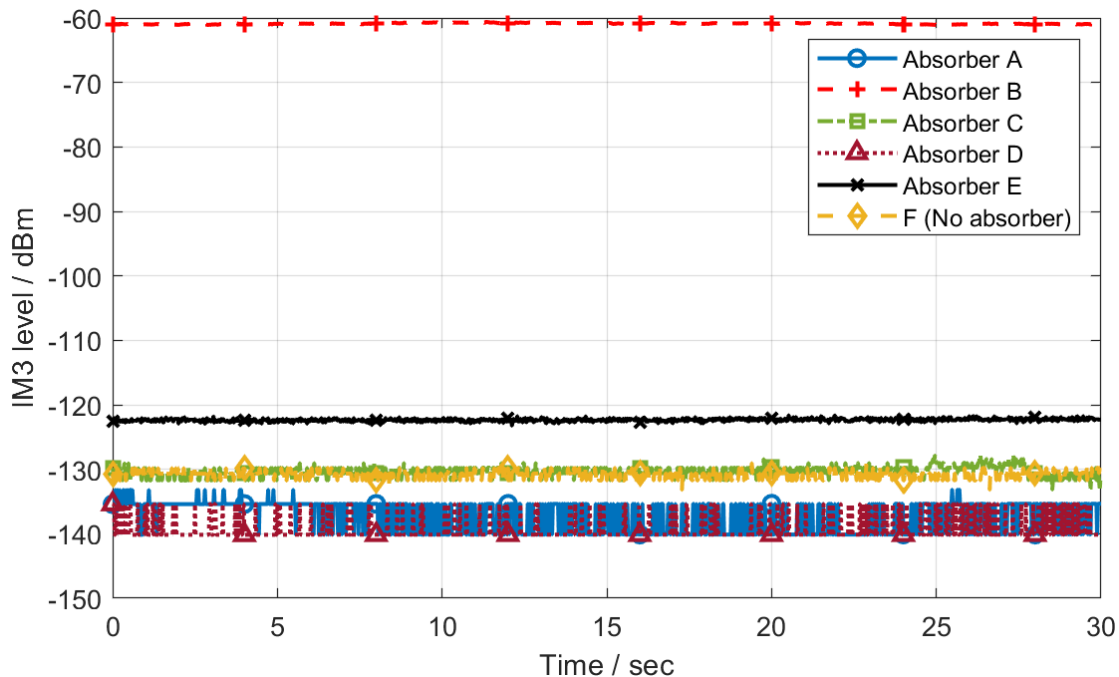


Fig. 3. PIM versus time at 43 dBm two-tone power, tone#1 frequency is 2110 MHz, tone#2 frequency is 2170 MHz and 3rd PIM product frequency is 2050 MHz.

The PIM produced from absorber 'A' and absorber 'D' is slightly lower than the measured residual PIM of the measurement setup 'F' shown in Fig. 3. This behavior can be due to the absorption of the residual PIM by the tested absorbers during the measurement.

Results of PIM versus Time at Variable Positions

In a next step the influence of the distance between antenna and the tested absorber is evaluated. The measurement setup remains unchanged and only the tested samples are moved from one position to another. The two-tone power is set at 43 dBm each. The average PIM of each AUT is then calculated at each position. Fig. 4 shows the average PIM versus the distance between the antenna radiating surface and the tip of the AUT. The PIM produced from 'A', 'E', and 'D' absorbers decreases, as the distance between the antenna and the AUT increases.

As expected, the measured PIM increases as the distance between the antenna and AUT decreases as shown in Fig. 4. This behavior can be due to the reduction of two-tone power as the distance between the antenna and the tested absorbers becomes larger and also the measured PIM signal becomes lower as the PIM source moves far from the antenna due to free space attenuation.

Fig. 4 shows that the PIM of Absorber 'C' has slightly decreased when it is moved from Position #1 to Position #2. However, the measured PIM of 'C' in Position #3 is almost the same level as in Position #2. Absorber 'B' behaves differently, and this might be resulted due to the absorbent material type used in fabricating this AUT. In general, the measured PIM level becomes lower as the PIM source is moved further away from the antenna.

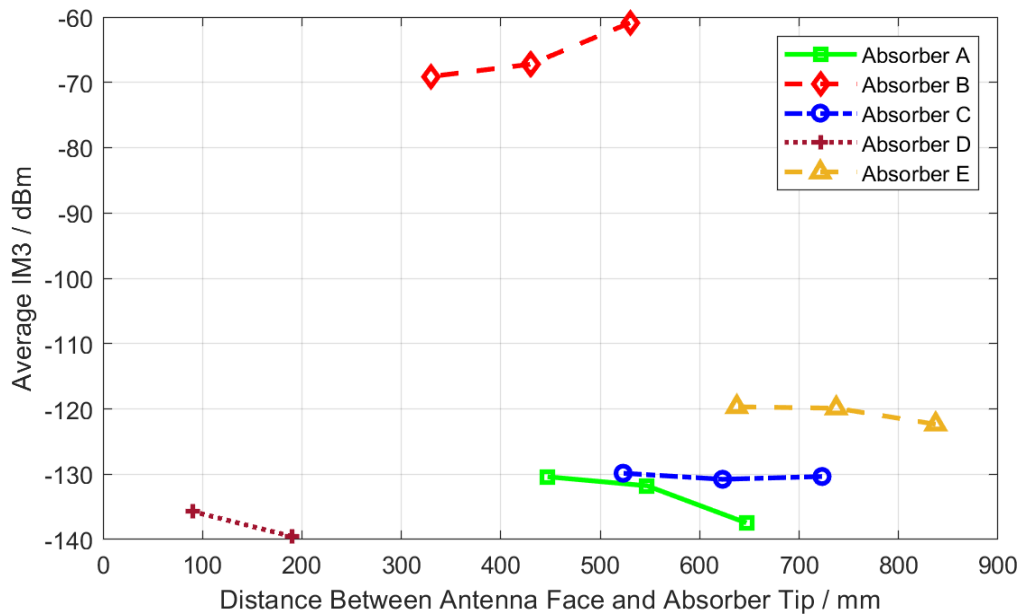


Fig. 4. Average PIM versus distance between antenna and absorber tip at 43 dBm two-tone power, tone#1 frequency is 2110 MHz, tone#2 frequency is 2170 MHz and 3rd PIM product frequency is 2050 MHz.

The power flux density on the absorber material can be estimated based on the antenna gain, input power to the antenna and the distance between the absorber footprint and the radiating antenna face. The antenna gain is 17.5 dBi and the transmitted carrier-power is 43 dBm. The distances between the antenna radiating surface and the absorber base are 850 mm, 750 mm and 650 mm for Positions #1, #2 and #3, respectively. So, the power flux densities assuming radiation into free space would be 247.7 W/m², 318.2 W/m², 423.7 W/m² at Positions #1, #2 and #3 respectively.

Results of PIM versus Power Sweep at Position#1

The absorber sample 'A' is attached to the ceil of the holding structure at Position #1 and the PIM versus power sweep is measured. The same process is repeated for all the AUTs using the same measurement setup. Fig. 5 shows that absorber 'A' and absorber 'D' materials produce low PIM level close to the residual PIM level of the measuring system. The produced PIM of absorbers 'A' and 'D' increases when the two-tone power reaches 44 dBm with approximate slope of around 2.66 and 2.9 respectively as shown in Table 2. Absorber 'C' and absorber 'E' material produce low PIM level slightly greater than the residual PIM level as depicted in Fig. 5. However, the generated PIM of these absorbers increases rapidly as the two-tone power increases from 43 dBm to 46 dBm with approximate slope of 3.53 and 3 respectively. Absorber 'B' has different behavior in response to the two-tone power. It produces PIM even when the two-tone power is low as depicted in Fig. 5 (a).

Table 2. Approximate slope of PIM increasing as two-tone power increases.

Absorber	A	B	C	D	E
Approx. slope	2.66	1.96	3.53	2.9	3

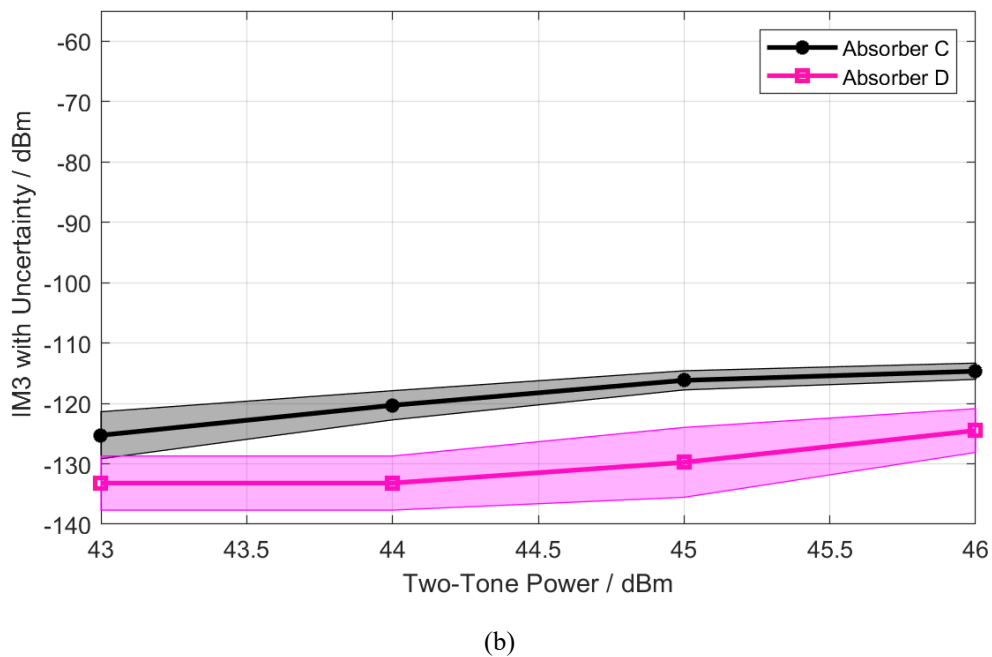
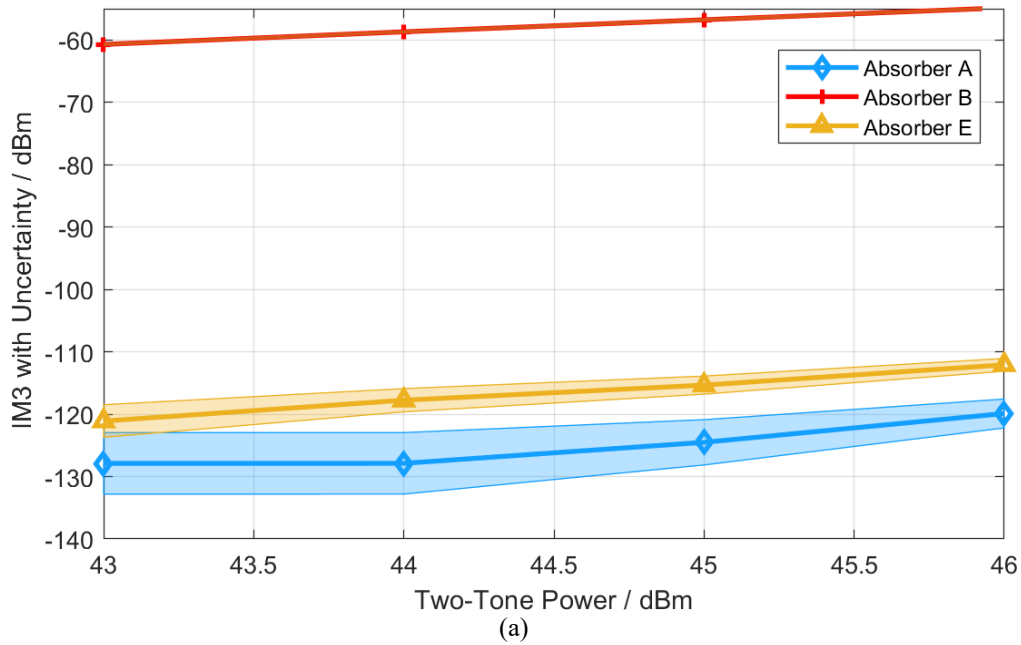


Fig. 5. PIM versus power sweep with uncertainty at Position #1 at tone#1 frequency is 2110 MHz, tone#2 frequency is 2170 MHz and 3rd PIM product frequency is 2050 MHz.

Thus, the PIM produced from this absorber increases slightly over the two-tone power range from 43 dBm to 46 dBm with approximate slope around 1.96 dB per 1 dB increase of two-tone power as shown in Table 2. The approximate slope shown in Table 2 represents the increase of PIM level per 1 dB increase in two-tone power.

The uncertainty of the measured IM3 is calculated based on IEC 62037-1 standard. The uncertainty contributors are the uncertainty of power meter (PM) used for calibrating the two-tone power, 30 dB RF attenuator uncertainty, uncertainty of signal generator used for calibrating the PIM receiver and the errors associated with the difference between the measured PIM and the residual PIM level. In this measurement, the dominant contributor to the uncertainty is the error related to the difference between the measured PIM level and the residual PIM level. So, the measured PIM levels near to the residual PIM had higher uncertainty as shown in Fig. 5.

Fig. 5 reveals that the PIM level produced from absorber 'A' has high uncertainties with almost ± 4.9 dBm at 43 dBm, and ± 2.3 dBm at 46 dBm of two-tone power. The PIM produced from absorber 'B' material has an uncertainty of ± 0.13 dBm over the two-tone power range from 43 dBm to 46 dBm. The measured PIM produced from absorber 'C' material is ± 3.9 dBm at 43 dBm and ± 1.35 dBm at 46 dBm of two-tone power. The uncertainty of the measured PIM produced from absorber 'E' is 2.6 dBm at 43 dBm and 1 dBm at 46 dBm of two-tone power as portrayed in Fig. 5.

CONCLUSION

In this paper, the PIM-performance of five different kinds of absorbers is investigated. It is confirmed that RF absorbers can produce significant levels of PIM, which may affect the accuracy of PIM measurements for RF radiating components in anechoic chambers. So, it is important to evaluate PIM performance of RF absorbers at sufficient two-tone power before performing actual PIM measurements using them. Also, the measured PIM level decreases as the distance between the radiating antenna and the RF absorbers increases. So, it is important to be taken into the account during the design of anechoic chambers used for PIM measurement.

ACKNOWLEDGMENT

The authors thank the Federal Ministry for Digital and Transport, Germany (BMDV) for funding this project titled "5G-Reallabor in der Mobilitätsregion Braunschweig-Wolfsburg". We also acknowledge Mr. Ohms from deutsche Telekom for borrowing us the radiating antenna.

REFERENCES

- [1] D. U. C. Delgado, C. A. Gutierrez, and O. Caicedo, "5g and beyond: Past, present and future of the mobile communications," *IEEE Latin America Transactions*, vol. 19, no. 10, pp. 1702–1736, 2021.
- [2] S. Mumtaz, J. M. Jornet, J. Aulin, W. H. Gerstacker, X. Dong, and B. Ai, "Terahertz communication for vehicular networks," *IEEE Transactions on Vehicular Technology*, vol. 66, no. 7, 2017.
- [3] R. Butler, "PIM testing- Advanced wireless services emphasize the need for better PIM control," *White Paper CommScope*, 2017.
- [4] D. S. Kozlov, A. P. Shitvov, A. G. Schuchinsky, and M. B. Steer, "Passive intermodulation of analog and digital signals on transmission lines with distributed nonlinearities: Modelling and characterization," *IEEE Transactions on microwave theory and techniques*, vol. 64, no. 5, pp. 1383–1395, 2016.
- [5] International Electrotechnical Commission, "Passive RF and microwave devices, intermodulation level measurement part 1: General requirements and measuring methods", 2012.
- [6] P. L. Lui, "Passive intermodulation interference in communication systems," *Electronics Communication Engineering Journal*, vol. 2, pp. 109–118, June 1990.
- [7] X. Chen and Y. He, "Reconfigurable Passive Intermodulation Behavior on Nickel-Coated Cell Array," *IEEE Transactions on Electromagnetic Compatibility*, vol. 59, pp. 1027–1034, Aug 2017.
- [8] J. T. Kim, I.-K. Cho, M. Y. Jeong, and T.-G. Choy, "Effects of external PIM sources on antenna PIM measurements," *ETRI journal*, vol. 24, no. 6, pp. 435–442, 2002.
- [9] Z. Cai, Y. Zhou, L. Liu, F. de Paulis, Y. Qi, and A. Orlandi, "A method for measuring the maximum measurable gain of a passive intermodulation chamber," *Electronics*, vol. 10, no. 7, p. 770, 2021.
- [10] Z. Cai, Y. Zhou, L. Liu, Y. Qi, W. Yu, J. Fan, M. Yu, and Q. Luo, "Small anechoic chamber design method for on-line and on-site passive intermodulation measurement," *IEEE Transactions on Instrumentation and Measurement*, vol. 69, no. 6, pp. 3377–3387, 2019.
- [11] G. Nimitz and U. Panten, "Broad band electromagnetic wave absorbers designed with nano-metal films," *Annalen der Physik*, vol. 19, no. 1-2, pp. 53–59, 2010.